Electronic Supplementary Material (ESI) for Journal of Materials Chemistry A.

Supporting Information

Hierarchical Multicarbonyl Polyimide Architectures as Promising Anode Active Materials for High-Performance Lithium/Sodium Ion Batteries

Jun Li[#a], Mo Luo[#b], Zhaohu Ba[a], Zhenxing Wang[a], Lijuan Chen[a], Yingzhi Li[c], Mengmeng Li[a], Hai-Bei Li[b], Jie Dong[a], Xin Zhao[a*] and Qinghua Zhang[a*]

a. State Key Laboratory for Modification of Chemical Fibers and Polymer Materials, College of Materials Science and Engineering, Donghua University,
Shanghai 201620, PR China

b. School of Ocean, Shandong University, Weihai 264209, PR China

c. Southern University Science and Technology, Department of Materials Science and Engineering, Shenzhen 518055, PR China

Corresponding author: xzhao@dhu.edu.cn, qhzhang@dhu.edu.cn

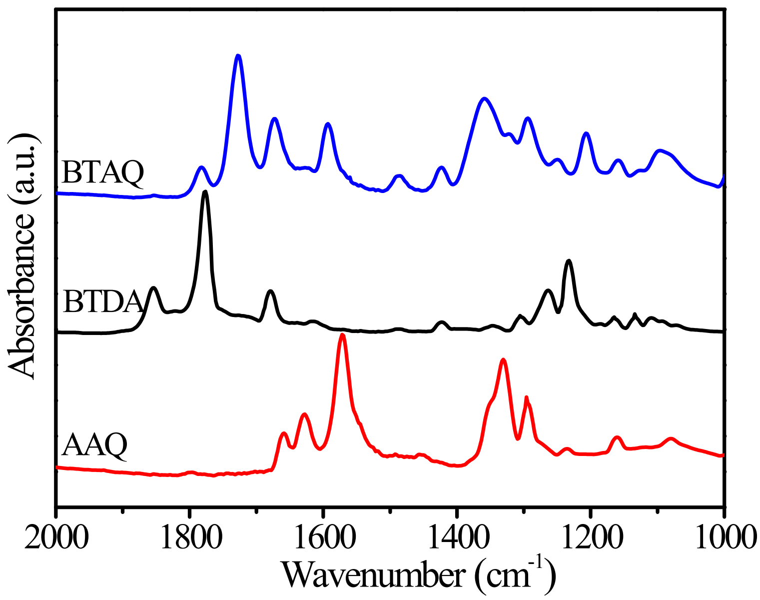

Figure S1. FTIR spectra of BTAQ with each monomer.

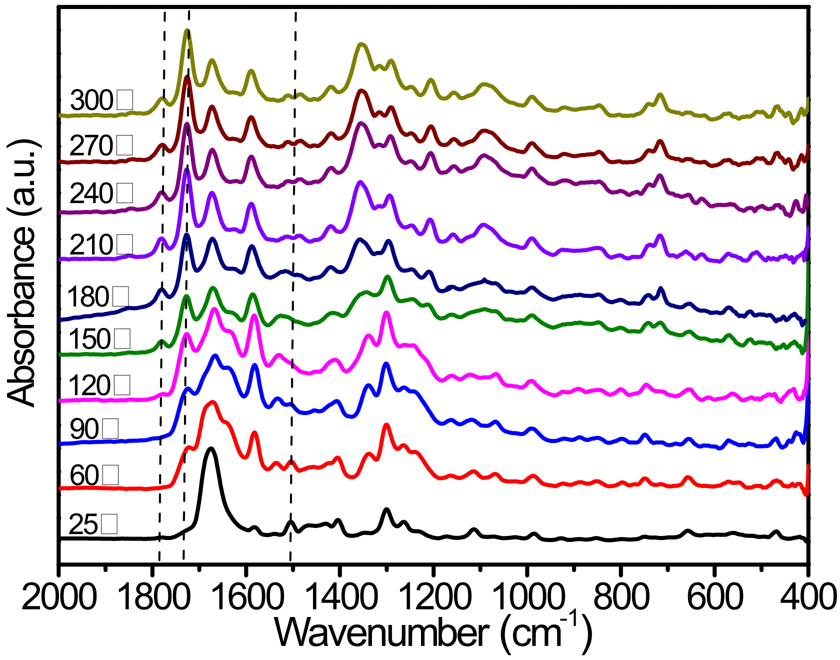

Figure S2. Temperature-programmed infrared spectroscopy of BTAQ

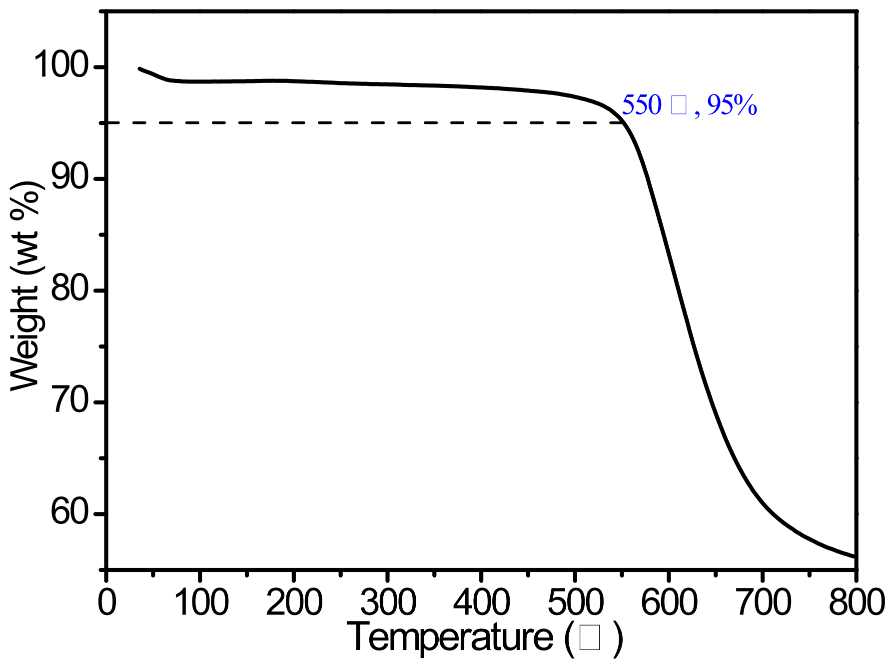

Figure S3. The TGA curves of BTAQ

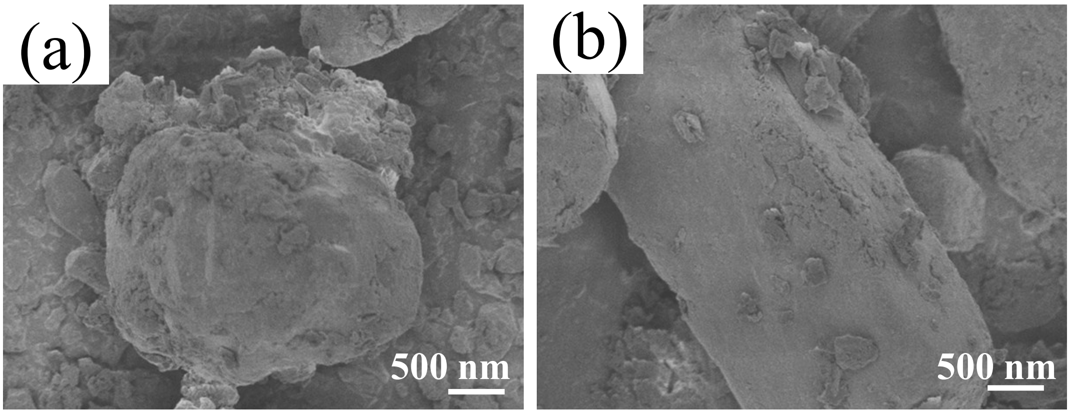

Figure S4. SEM image of (a) BTDA and (b) DAAQ

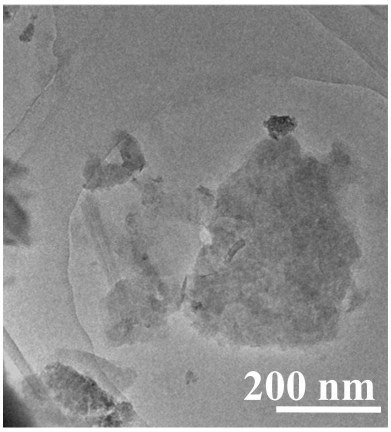

Figure S5. TEM image of BTAQ after sonication in ethanol.

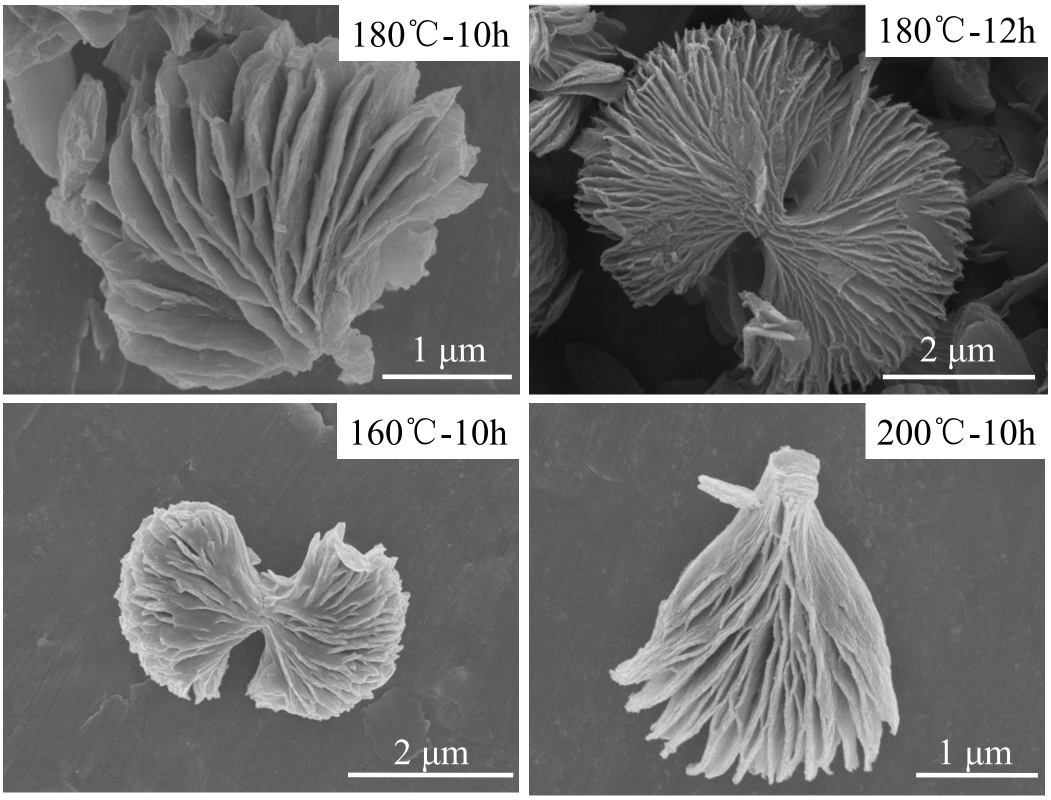

Figure S6. SEM images of different samples obtained with various reaction conditions

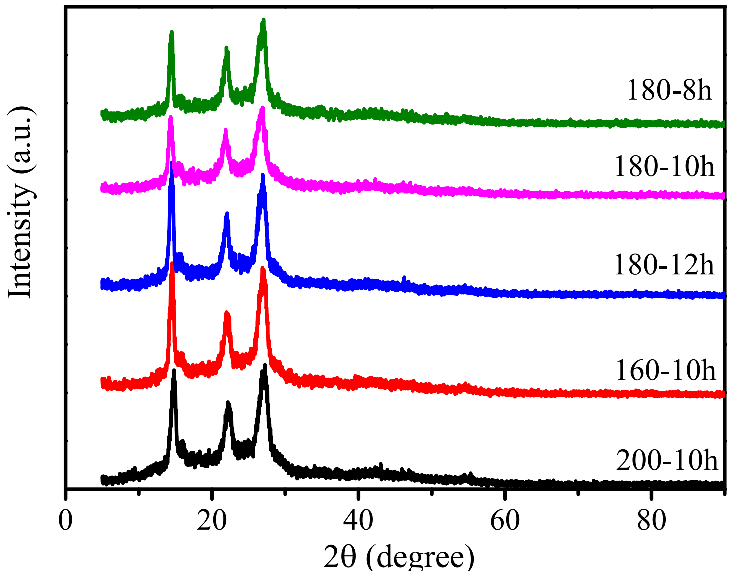

Figure S7. XRD curves of the products obtained with different reaction conditions

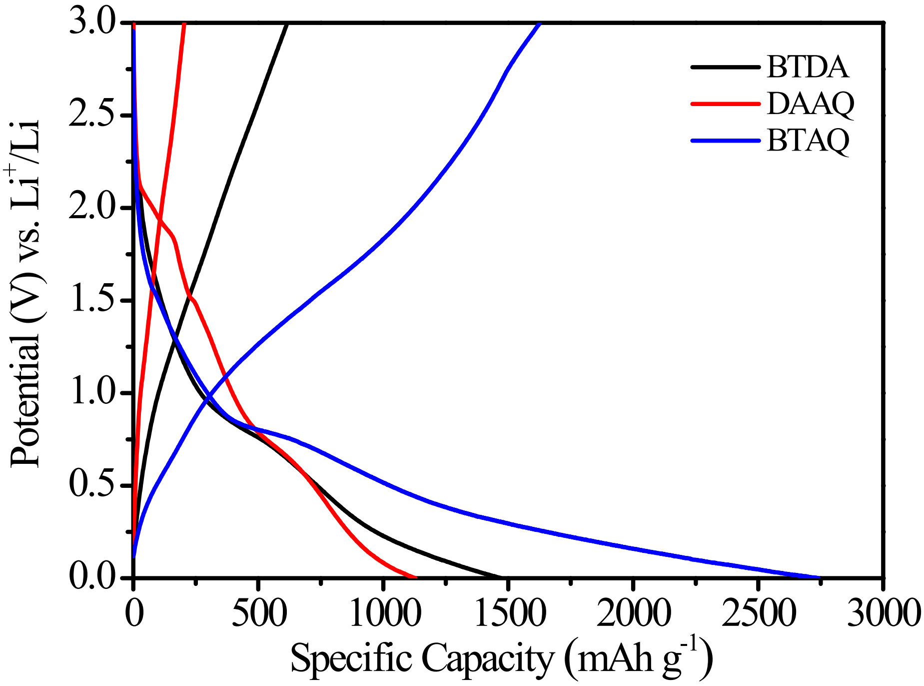

Figure S8. Charge-discharge profiles of monomers and BTAQ at the initial cycle a current density of 0.1 A g^{-1}

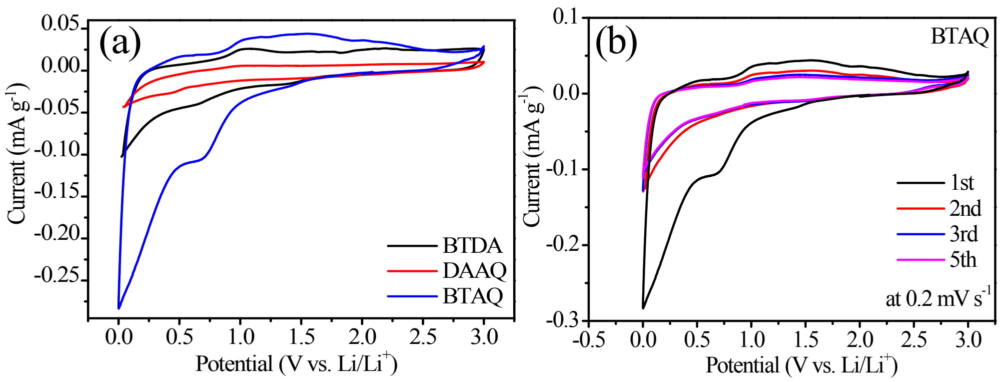

Figure S9. (a) The CV profiles of each monomer and BTAQ, (b) the CV curves of BTAQ at the first five cycles with a scan rate of 0.2 mV s^{-1}.

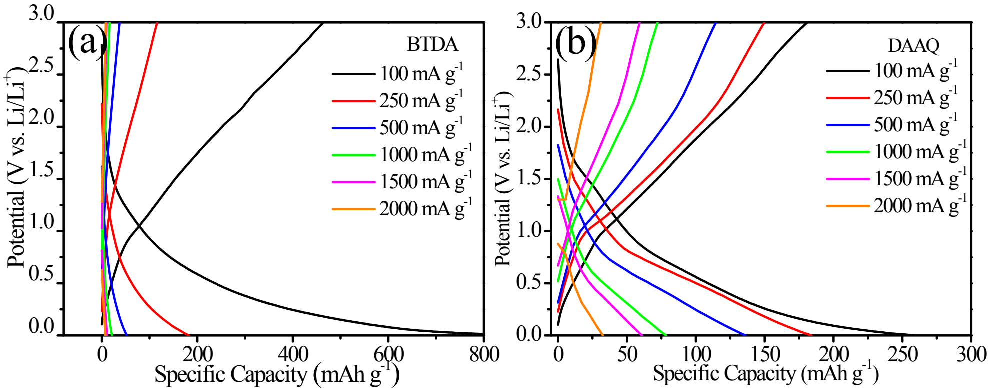

Figure S10. The charge-discharge curves of (a) BTDA and (b) DAAQ at various current densities.

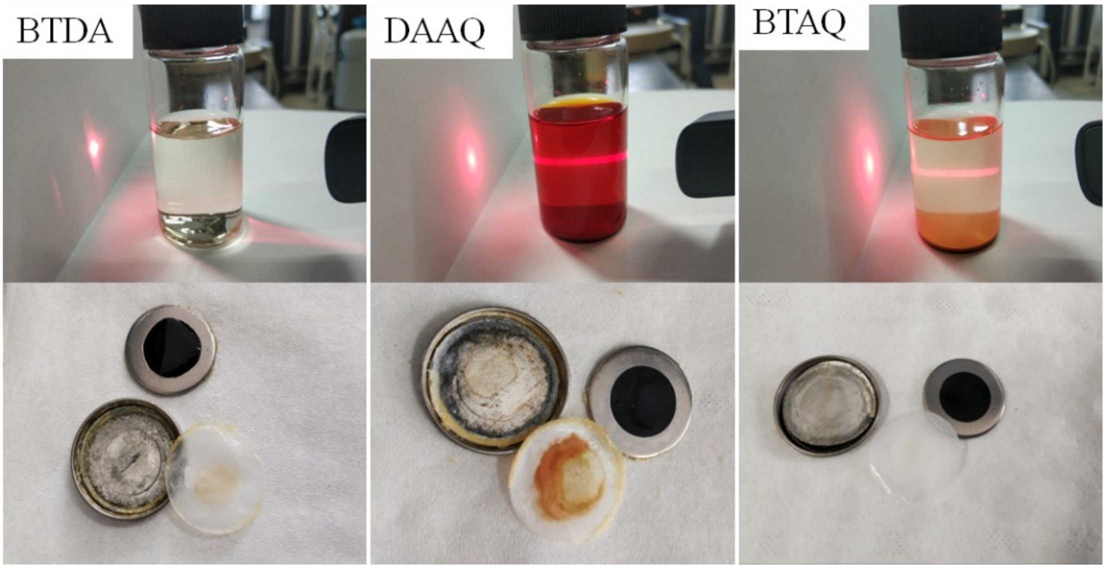

Figure S11. The dissolution properties of BTDA, DAAQ and BTAQ after cycling in electrolyte and the appearance of separator after cycling test.

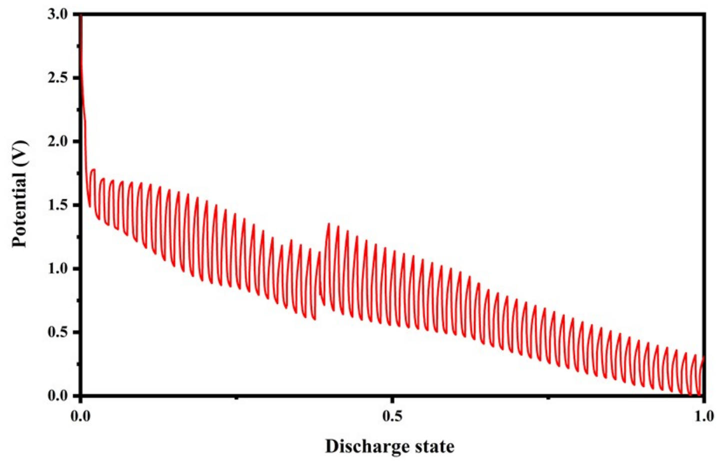

Figure S12. The GITT curves for BTAQ electrode

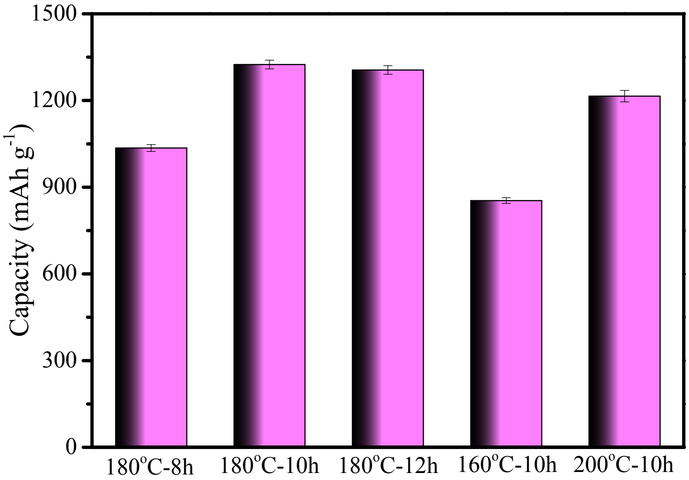

Figure S13. The average specific discharge capacities of BTAQ by various reaction conditions

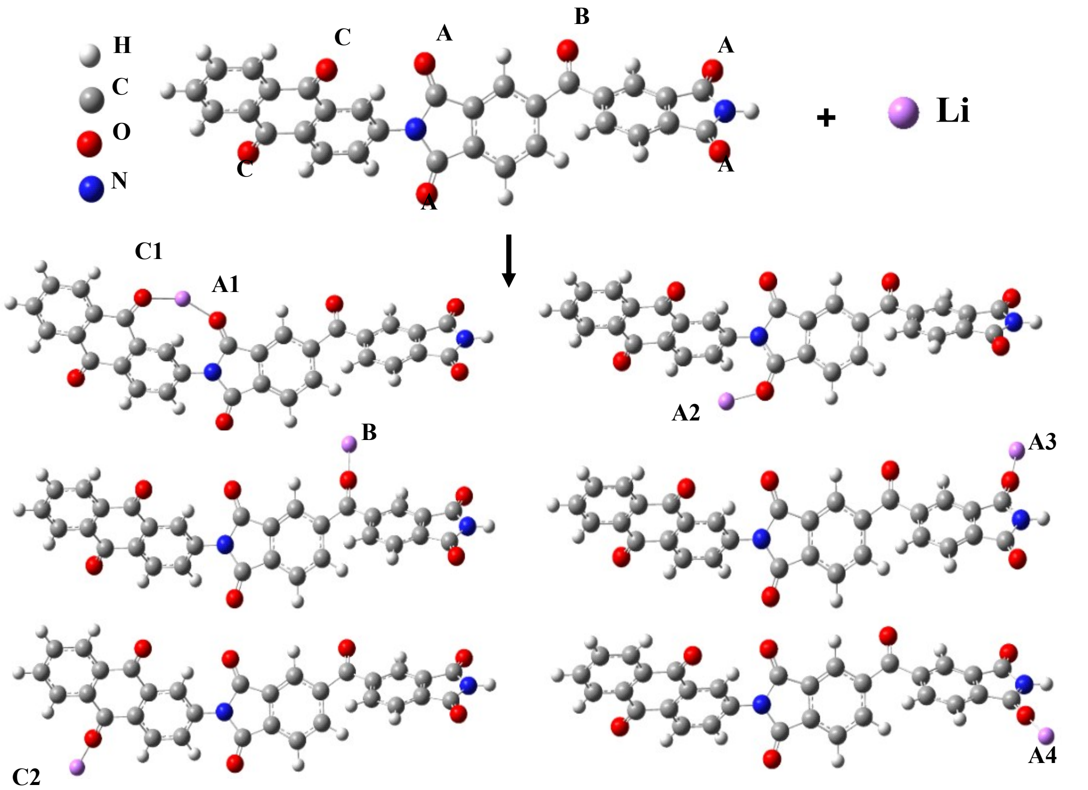

Figure S14. The diagrams of simulated combination for different active sites with Li species.

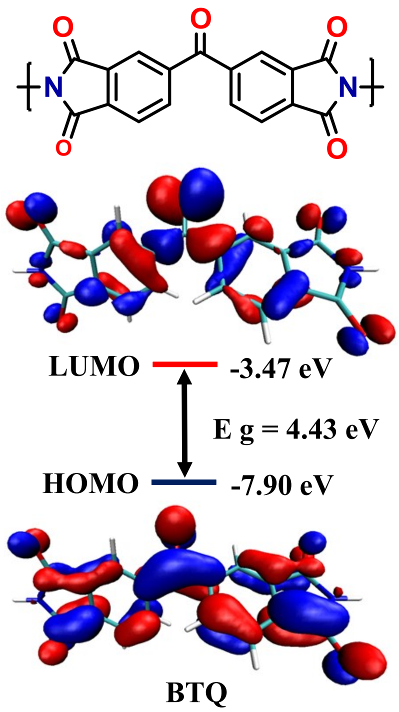

Figure S15. Energy level diagram for structure of BTQ obtained from DFT calculations.

Table S1. Elemental analysis of BTAQ and each monomer

	Calculated values %					Theoretical values %				
	C	H	O	N	N:O	C	H	O	N	N:O
BTDA	62.95	1.9	35.15	—	—	63.31	1.86	34.78	—	—
DAAQ	70.17	4.13	13.98	11.72	0.84	70.59	4.2	13.15	11.76	0.89
BTAQ	69.56	2.43	22.66	5.35	0.24	70.99	2.29	21.37	5.34	0.25

Table S2. Comparison with the reported results of organic anode materials for LIBs

Anode materials	Specific capacity ($mAh\ g^{-1}$)	Capacity after cycling test ($mAh\ g^{-1}$)	Number of cycles	Refs
BTQ	1001@42 mA g^{-1}	829@42 mA g^{-1}	50	*Small* **2018**, *14*, 1704094
BLL	662@192.6 mA g^{-1}	619@100 mA g^{-1} (RT)	50	*Adv. Energy Mater.* **2015**, *5*, 1402189
	1416@192.6 mA g^{-1}	1181 @100 mA g^{-1} (50℃)		
CIN-1/CNT	-	292@100 mA g^{-1}	250	*Adv. Energy Mater.* **2019**, *9*, 1801010
SNW-1/CNT	-	306@100 mA g^{-1}		
ECIN-1/CNT	1269@100 mA g^{-1}	749@100 mA g^{-1}		
ESNW-1/CNT	1470@100 mA g^{-1}	693@100mA g^{-1}		
PAT-COF	1305@100mA g^{-1}	1770@200mA g^{-1}	400	*ACS Appl. Mater. Interfaces* **2018**, *10*, 37023
Benzenetricarboxaldehyde-based COF@CNT	928@100 mA g^{-1}	1032@100 mA g^{-1}	500	*Nat. Comm.*, **2018**, *9*, 576
PSB	315@10 mA g^{-1}	160@10 mA g^{-1}	100	*Electrochim. Acta*, **2017**, *253*, 319
PIAQ	1130@200 mA g^{-1}	1097@200 mA g^{-1}	100	*J. Mater. Chem. A*, **2019**, *7*, 2368
PI	192@100 mA g^{-}	176@100 mA g^{-1}	100	*J. Mater. Chem. A*, **2018**, *6*, 21216
PI-MG	783@100 mA g^{-1}	612@100 mA g^{-1}		
BTAQ	**1343.8@100 mA g^{-1}**	**665.1@250 mA g^{-1}**	**50**	**This work**

Table S3. Comparison with the reported results of anode materials for SIBs

Anode materials	**Specific capacity ($mAh\ g^{-1}$)**	**Capacity after cycling test ($mAh\ g^{-1}$)**	**Number of cycles**	**Ref**
TAPB-terephthalaldehyde COF	303@100 mA g^{-1}	300@100 mA g^{-1}	1000	*Electrochim. Acta,* **2019**, *301*, 23
PMDA-MA COF	1312@100 mA g^{-1} 137@10 A g^{-1}	130@ 10 A g^{-1}	1000	*ACS Nano*, **2019**, *13*, 2473
Carbon/graphene composite	170@500 mA g^{-1}	142@500 mA g^{-1}	2500	*Nano Energy*, **2015**, *12*, 224
Hollow carbon nanospheres	171@500 mA g^{-1}	160@100 mA g^{-1}	100	*Adv. Energy Mater.*, **2012**, *2*, 873
Carbon nanofibres	296@500 mA g^{-1}	243@50 mA g^{-1}	100	*Nanoscale*, **2014**, *6*, 1384
PMDA-PDA	124@50 mA g^{-1}	125@24 mA g^{-1}	100	*Electrochim. Acta*, **2018**, *265*, 702
BTAQ	**275.8@25 mA g^{-1}**	**130@25 mA g^{-1}**	**100**	**This work**